![Texas Instruments logo]

Sensorless Stall Detection With the DRV8889-Q1

Dipankar Mitra

ABSTRACT

A stepper motor system is essentially an open-loop position control system. There is no feedback to let the driver IC know if the motor is running or stalled. However, in many applications, the user needs to know the status of the motor – either for diagnostics purpose or for position sensing. Sensorless stall detection solutions available in the market today do not detect stall reliably across wide range of operating parameters such as supply voltage, temperature, and micro-stepping modes. Texas Instruments' DRV8889-Q1 device implements a novel approach towards sensorless stall detection of stepper motors by using the PWM OFF-time to sense the back EMF. This stall detection algorithm eliminates first-order dependency on supply voltage, coil resistance, and temperature changes. The goal of this application report is to highlight the advantages of the stall detection algorithm of the DRV8889-Q1 and provide examples of how the DRV8889-Q1 can detect stall reliably in a wide variety of end applications.

Contents

List of Figures

List of Tables

Trademarks

All trademarks are the property of their respective owners.

1   Need for Sensorless Stall Detection

The simplicity of the open-loop stepper motor system is attractive; however, even in a stepper motor, feedback can be desirable. Many applications require the system to know the state of the motor either for diagnostics purposes, such as being able to detect if the motor is jammed or overloaded; and also for position sensing - to be able to detect if the motor has reached the end of line or hit a physical obstruction.

Applications often severely over-drive the motor beyond the desired end point to ensure the end point is reached, reducing the efficiency of the system. External components to monitor motor position, such as encoders or Hall sensors add cost to the system. Without stall detection, the motor driver will continue to drive through the obstacle; causing audible noise and mechanical failures.

An integrated sensorless stall detection method can address these negative effects and ensure that the motor is not overloaded or obstructed. Moreover, in situations where precise position sensing is not required, sensorless stall detection can replace expensive Hall sensors, limit switches, and encoders. Integrated sensorless stall detection also provides immediate response when a stall occurs compared to the position sensor solution which requires a timeout mechanism.

A few of the systems and applications which can benefit from an integrated sensorless stall detection algorithm are:

*   Automotive headlight leveling and swivel
*   Automotive Head-Up Display (HUD)
*   Automotive and Industrial HVAC actuator control
*   Electronic Expansion Valves (EEV)
*   Multi-function printers
*   3-D printers
*   ATMs
*   Textile machines
*   Surveillance cameras (pan and tilt motion)

2   Back EMF for a Stepper Motor

For a stepper motor, the supply voltage can be expressed with Equation 1:

$$VM = I \times R_{coil} + BEMF + L \times \frac{di}{dt}$$

where

*   I is the coil current
* R_{coil} is the coil resistance of the motor coil
*   BEMF is the back-EMF voltage
*   L is the inductance of the coil   (1)

The back EMF is the voltage generated by the motor as the armature spins inside the stator. The back EMF can be expressed using Equation 2:

$$BEMF = -p \times \psi_m \times \omega \times \sin(p\omega t)$$

where

*   p is the number of pole pairs
* ψ_m is the maximum magnetic flux of the motor
* ω is the angular speed of the motor
* ψ_m are constants specific to each motor   (2)

Therefore, the back EMF is sinusoidal in nature and directly proportional to the motor speed (ω). A motor, when spinning fast, will produce more back EMF than when spinning slower. And when the motor is stalled, no back EMF is produced.
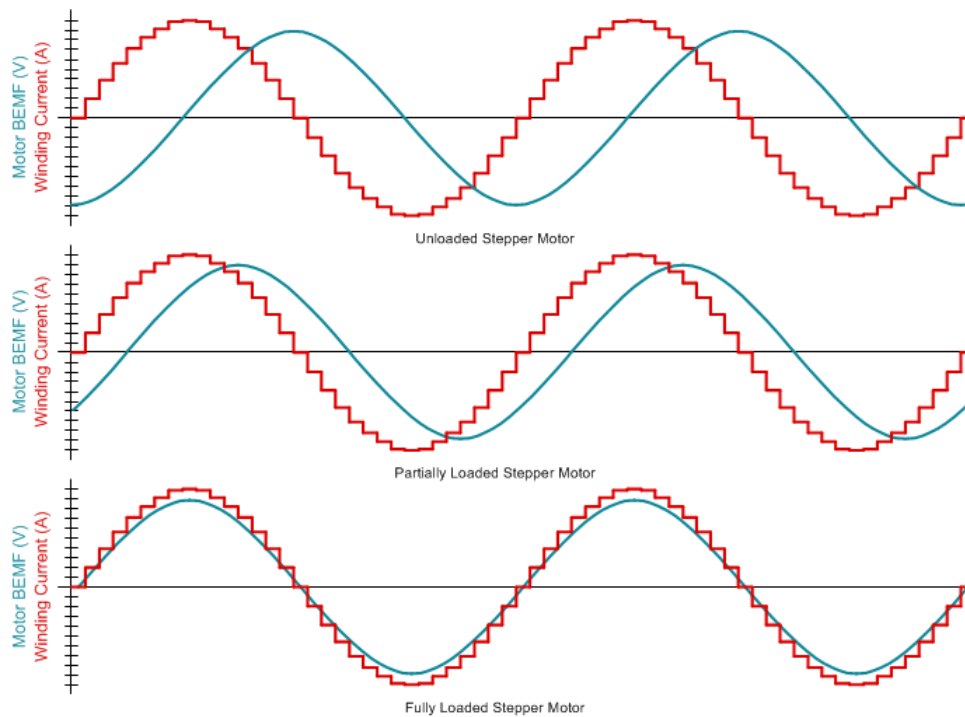
Figure 1. Back-EMF Phase Shift With Coil Current

Stepper motors have a distinct relation between the coil current, back EMF, and mechanical torque load of the motor, shown in Figure 1. Compared to the coil current, the back EMF will be phase-shifted by 90° for an unloaded motor. As the motor load approaches the torque capability of the motor at a given coil current, the back EMF moves in phase with the coil current. When the load torque increases beyond the fully-loaded condition, the rotor falls out of synchronization with the stator magnetic field, causing the motor to stall.

The maximum torque that can be applied to a motor operating at a given speed without losing synchronization is called the pull-out torque. Therefore, a stall condition occurs when the load torque on a motor exceeds the pull-out torque of the motor. Most stepper motor data sheets include pull-out torque vs. speed curves. The pull-out torque will decrease as the speed increases and increase as the current through the motor coils increases.

3 Existing Sensorless Stall Detection Algorithms

Multiple sensorless stall detection algorithms are available today from various stepper driver manufacturers. A short description of those methods follows:

3.1 Measuring Back EMF During Current Zero Cross

Most stall detection algorithms currently available in the market measure back EMF during sinusoidal current zero crossing. When the coil current is zero, the voltage across the motor coil is equal to the back EMF. As the motor stalls, the back EMF drops to a value close to zero. Therefore, when the back EMF decreases, it gives a good indication that the motor has stalled.

However, this method has certain drawbacks, such as:

1. Back EMF is only monitored during zero crossing.
2. The measurement window needs to ensure that the coil current has really reached zero. Ringing in the coil voltage waveform around the zero crossing can shorten the measurement window and extra blanking time might be needed.
3. For high motor speeds, this method needs complicated circuitry for fast measurement. So, this method does not work above moderately high motor speeds.

4. This method does not work in *Full Step* mode - coil current switches between 71% and –71% of full-scale setting in full-step mode; therefore, zero-cross detection is not possible. Some algorithms force a zero-cross period even in full-step mode - but that approach has its own issues.

5. When the motor is spinning slowly, the change in back EMF can be hard to detect.
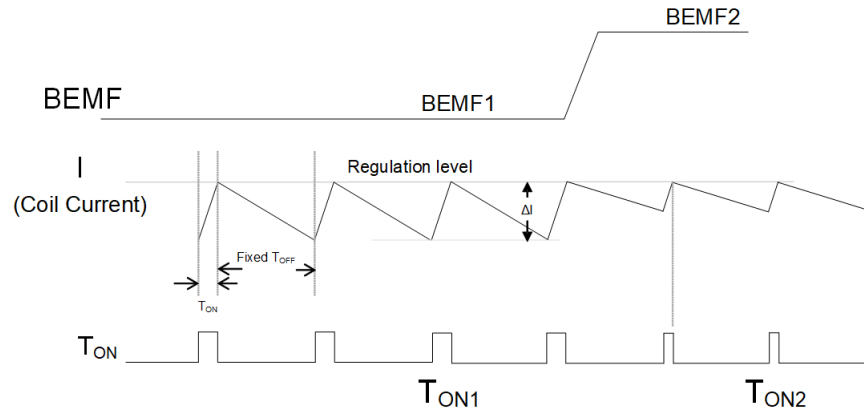
3.2 *Constant OFF-time Method*

Figure 2. Fixed OFF-time Method

Some fixed PWM OFF-time (T_{OFF}) current regulation methods depend on the difference between PWM on times (T_{ON}) in successive cycles to determine back EMF and therefore detect stall, as Figure 2 shows.

However, this method has its own drawbacks as well. The equation for the on time follows:

$$T_{ON} = T_{OFF} \times \frac{\left(\left(I \times R\right) - BEMF\right)}{\left(VM - \left(\left(I \times R\right) - BEMF\right)\right)}$$
(3)

$$\Delta T_{ON} = T_{ON1} - T_{ON2} = T_{OFF} \times \frac{VM \times \left(BEMF2 - BEMF1\right)}{\left(VM - \left(\left(I \times R\right) - BEMF1\right)\right) \times \left(VM - \left(\left(I \times R\right) - BEMF2\right)\right)}$$
(4)

As is evident from Equation 4, ΔT_{ON} depends on supply voltage, coil current and coil resistance (and therefore ambient temperature). So, this algorithm can potentially result in false and missed stall detection when supply voltage, temperature, or motor current changes.

3.3 *PWM Cycle-Counting Method*

Some implementations monitor PWM cycle count to sense back EMF changes, and thereby detect stall. Back EMF decreases at stall condition, allowing faster current rise time. At fixed step frequency, stall results in more PWM cycles per step (due to fixed T_{OFF}). Drawbacks of this method are:

1. As can be seen from Equation 3, T_{ON} is going to vary based on supply voltage (VM), motor current (I), and temperature (T) (motor resistance R increases with T). Therefore, this method might result in false and missed stall detection when the supply voltage, temperature, or motor current changes.

2. Does not work in Full Step mode

3. Works only when the step frequency is relatively constant. If the step frequency changes dynamically, it creates uncertainty in the number of PWM pulses.

4 DRV8889-Q1 Stall Detection Algorithm

4.1 Algorithm Details

Figure 1 shows that for an unloaded motor, back EMF is 90º phase shifted from the motor current. As the load increases, the back-EMF phase shift decreases. Finally, as the load increases to the point where the load torque exceeds the pull-out torque, the motor stalls and the back EMF goes to zero. By detecting back-EMF phase shift between rising and falling current quadrants of the motor current, the DRV8889-Q1 device can detect a motor overload stall condition or an end-of-line travel.
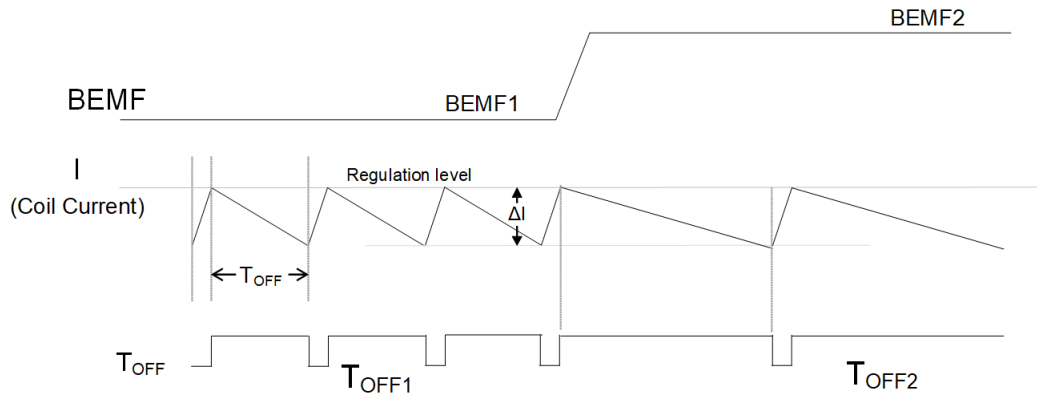

Figure 3. Fixed Ripple Current Method

$$T_{OFF} = \frac{L \times \Delta I}{(I \times R) - BEMF}$$

(5)

To overcome the issues associated with fixed T_{OFF} current regulation method, a fixed ripple current regulation method (smart tune ripple control decay mode) is used by the DRV8889-Q1, shown in Figure 3. This allows T_{OFF} to also vary based on back EMF in addition to T_{ON}. By monitoring T_{OFF} to detect back EMF changes, first order dependency on supply voltage is eliminated, as the supply is disconnected from the motor during T_{OFF}. Equation 5 shows that T_{OFF} does not depend on VM.

$$\frac{1}{T_{OFF1}} - \frac{1}{T_{OFF2}} = \frac{1}{L \times \Delta I} \times (BEMF2 - BEMF1)$$

(6)

Instead of T_{OFF} delta, the delta of the reciprocal of T_{OFF} can be used to further eliminate the dependency on I and R terms (motor current and resistance/temperature). As Equation 6 shows, delta ($1/T_{OFF}$) does not depend on VM, I, or R and only on back EMF change (other terms ΔI and L are current ripple and motor inductance which are constants for a system).

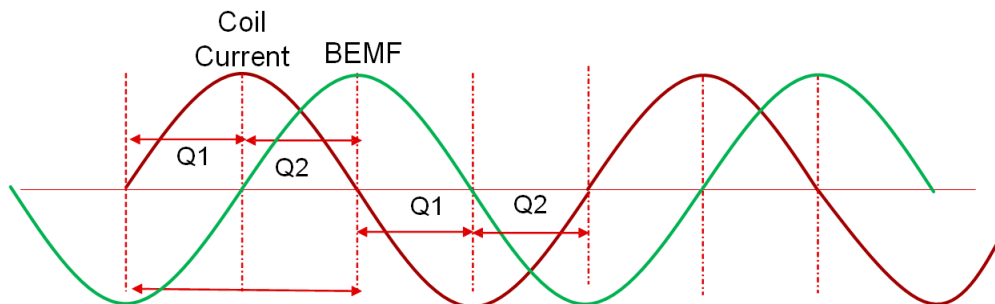**Figure 4. Back EMF for Unloaded Motor**

As Figure 4 shows, comparing the back EMF (by monitoring $1/T_{OFF}$) between the rising (Q1) and falling (Q2) current quadrants of the sinusoidal current can give a good indication of the motor load. For a lightly loaded motor, the delta back EMF between falling and rising quadrant in Figure 4 will be a positive value. As the load increases and approaches stall condition, the back-EMF delta between the falling and rising current quadrants will approach zero and can be used to detect the stall condition.

The algorithm used in the DRV8889-Q1 device monitors T_{OFF} during Q1 and Q2 of each electrical half-cycle. The subtraction between $1/T_{OFF1}$ (average) and $1/T_{OFF2}$ (average) happens at the end of each half-cycle. The $(1/T_{OFF1} - 1/T_{OFF2})$ value calculated at the end of a half-cycle is averaged with the values calculated at the end of three previous half-cycles, to arrive at a moving average called torque count, represented by the 8-bit register TRQ_COUNT (CTRL7 register in Table 1).

For a lightly loaded motor, the TRQ_COUNT is a non-zero value - call it steady count. As the motor approaches stall condition, TRQ_COUNT approaches zero (call it stall count) and can be used to detect the stall condition. If at anytime TRQ_COUNT falls below the stall threshold (represented by the 8-bit STALL_TH register), the device will detect stall.
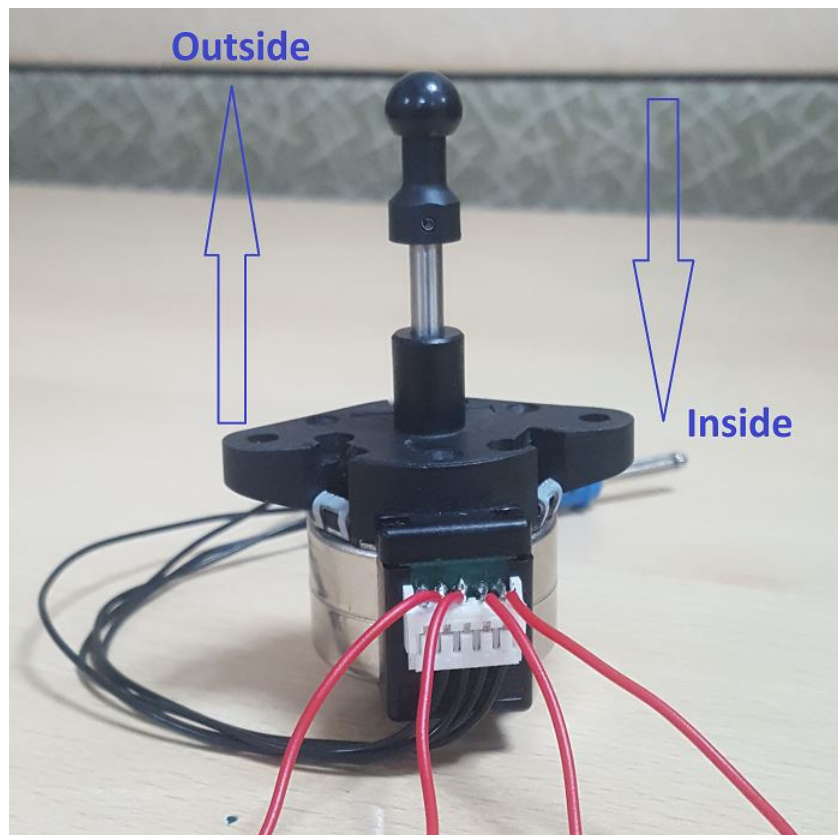
4.2   Torque Count Scope Shots

Figure 5. PL35L-024 Stepper Motor

The scope shots in this section are for a stepper motor commonly used in adaptive headlight applications - PL35L-024. It is rated for maximum 450 mA drive current and the coil has 7.7-Ω series resistance. Depending on the direction of motion, the motor shaft moves inside or outside, as shown in Figure 5.
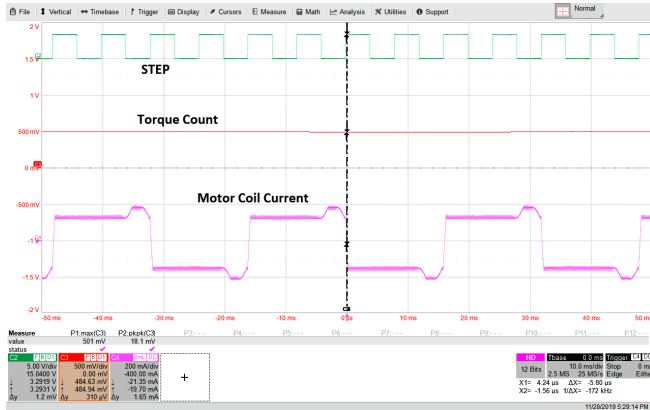
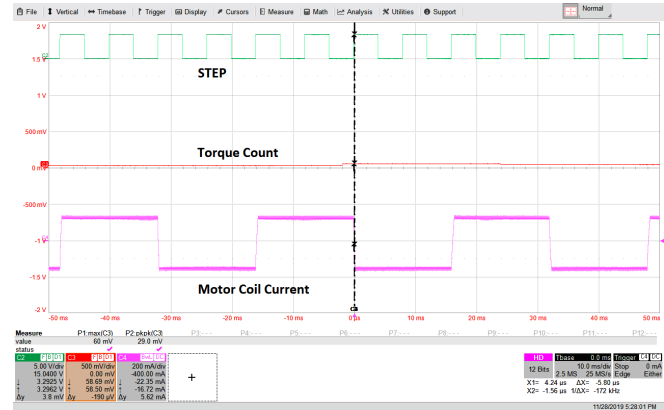**Figure 6. Coil Current and Torque Count When Motor is Running**

Figure 7. Coil Current and Torque Count When Motor is Stalled

On the DRV8889-Q1 EVM, the MSP430 MCU converts the TRQ_COUNT into an analog voltage, using the DAC inside the MCU. The full range of the DAC is 3.3 V, and it corresponds to 256 counts of the TRQ_COUNT register. Therefore, a single TRQ_COUNT bit is represented as 12.89 mV.

Figure 6 and Figure 7 show how the back EMF distorts the coil current when the motor is running. The supply voltage is 13.5 V, the DRV8889-Q1 device is set for full-step mode with 125 pps speed, 200 mA full-scale current, and 105 V/µs slew rate. The motor is stalled when the shaft moves to either end stop. When the motor is running at nominal speed, the presence of the back EMF causes the current to rise instead of decay during T_{OFF}, and the DAC output voltage is roughly 500 mV, corresponding to a TRQ_COUNT of 38. When the motor is stalled, there is no back EMF; therefore, the coil current stays uniform across quadrants, and the torque count falls to zero.
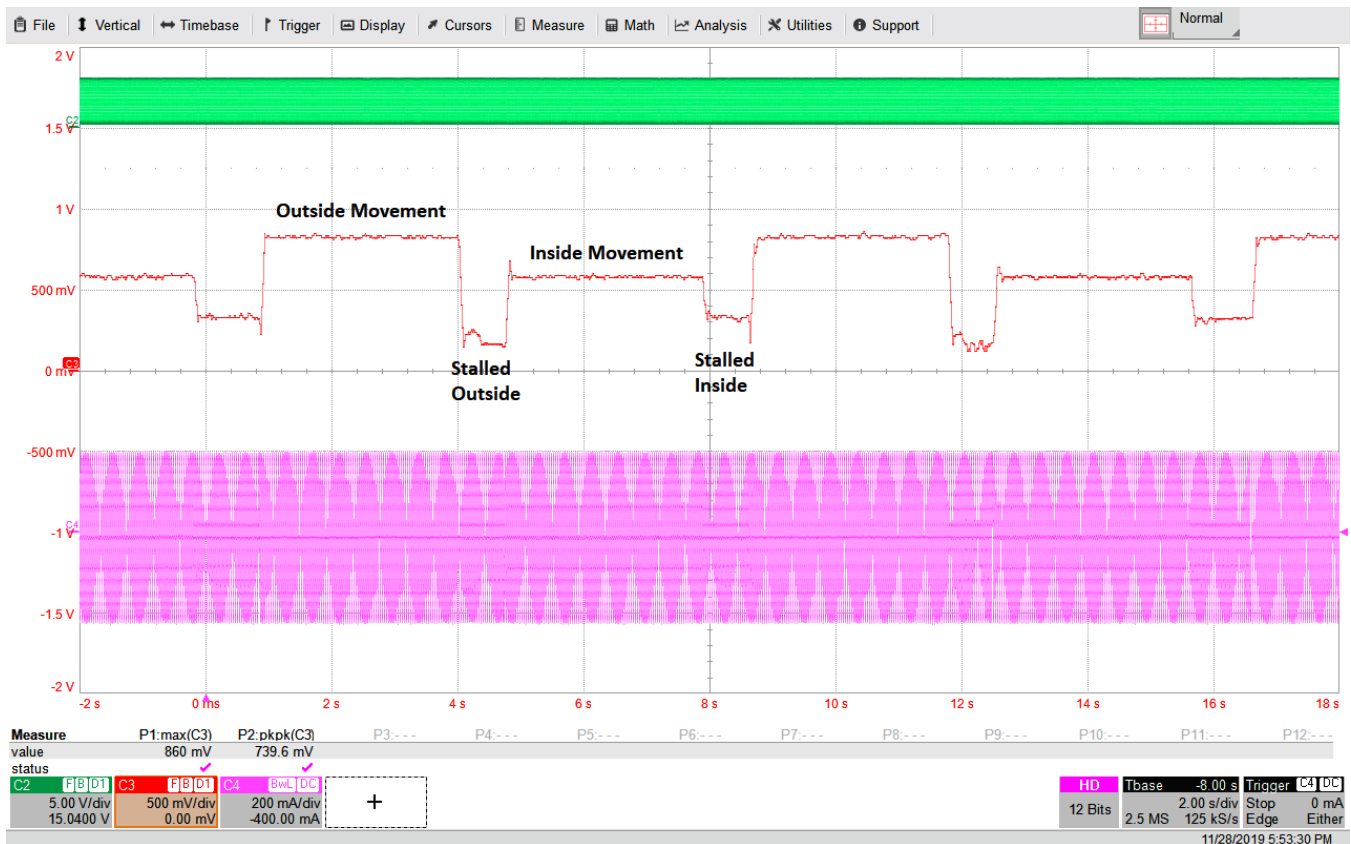

Figure 8. Torque Count of the PL35L-024 Motor

Figure 8 corresponds to the case where the motor shaft moves up and down continuously. It shows how the TRQ_COUNT value changes based on whether the rotor shaft is moving inside or outside, and whether it is stalled inside or outside. Users can set the stall threshold at a value midway between the lowest steady count and highest stall count. A STALL_TH of 35 (corresponding to 450 mV) will detect stall reliably irrespective of the direction of motion.

5 How to Configure the DRV8889-Q1 for Stall Detection

The *DRV8889-Q1 Evaluation Module User's Guide* details the hardware implementation of the EVM. Details on using the graphical user interface (GUI) software with this EVM are found in the DRV8889-Q1 EVM *DRV8889-Q1EVM GUI User's Guide*.

Table 1 lists the memory-mapped registers for the DRV8889-Q1 device.

Table 1. Memory Map

Register Name	7	6	5	4	3	2	1	0	Access Type	Address
FAULT Status	**FAULT**	SPI_ERROR	UVLO	CPUV	OCP	**STL**	TF	OL	R	0x00
DIAG Status 1	OCP_LS2_B	OCP_HS2_B	OCP_LS1_B	OCP_HS1_B	OCP_LS2_A	OCP_HS2_A	OCP_LS1_A	OCP_HS1_A	R	0x01
DIAG Status 2	UTW	OTW	OTS	**STL_LRN_OK**	**STALL**	RSVD	OL_B	OL_A	R	0x02
CTRL1	TRQ_DAC [3:0]				RSVD		SLEW_RATE [1:0]		RW	0x03
CTRL2	DIS_OUT	RSVD		TOFF [1:0]		**DECAY [2:0]**			RW	0x04
CTRL3	DIR	STEP	SPI_DIR	SPI_STEP	MICROSTEP_MODE [3:0]				RW	0x05
CTRL4	CLR_FLT	LOCK [2:0]			EN_OL	OCP_MODE	OTSD_MODE	TW_REP	RW	0x06
CTRL5	RSVD		**STL_LRN**	**EN_STL**	**STL_REP**	RSVD			RW	0x07
CTRL6	**STALL_TH [7:0]**								RW	0x08
CTRL7	**TRQ_COUNT [7:0]**								R	0x09

It is fairly easy to set up the device for stall detection with only a few bits controlling the critical parameters related to the stall detection algorithm. The bits relevant for stall detection follow and are highlighted in Table 1:

- **EN_STL [1:0]** in CTRL5 register: By default, stall detection is disabled after the device powers-up. EN_STL must be set to '1' to enable stall detection.
- **DECAY [2:0]** in CTRL2 register: The decay mode must be set to smart tune ripple control, therefore it must be ensured that DECAY [2:0] is set to '111'. Setting the decay mode to any other value will disable stall detection.
- **STL_LRN [1:0]** in CTRL5 register is '0' by default. It must be set to '1' to enable the automatic stall learning process. This bit automatically returns to '0' when the stall learning process is complete.
- **STL_LRN_OK [1:0]** in DIAG Status 2 register becomes '1' at the end of successful stall threshold learning.
- **TRQ_COUNT [7:0]** in CTRL7 register. An indicator of load torque - high when the motor is unloaded and close to zero when the motor is stalled.
- **STALL_TH [7:0]** in CTRL6 register. Can be programmed to the desired stall threshold level or can be set by the stall learning process. Anytime the torque count falls below the threshold, the device detects stall.
- **STL_REP [1:0]** in CTRL5 register has to be '1' to report stall detection fault on the nFAULT pin. In this case, nFAULT pin will be driven low when stall is detected. If STL_REP is '0', stall detection is not reported on nFAULT.

When stall is detected, the STALL, STL and FAULT bits are latched high and the nFAULT pin is pulled low (if STL_REP is '1'). In stalled condition, the motor shaft does not spin. However, the motor may still vibrate if the DRV8889-Q1 device continues to receive STEP signals. The coil current waveform is as shown in Figure 7, in that case.

The motor starts to spin again when the stall condition is removed. The nFAULT line is released and the fault registers are cleared when a clear faults command has been issued either through the CLR_FLT bit or an nSLEEP reset pulse.

6 How to set Stall Threshold

Stall threshold can be set in two ways, either write the STALL_TH bits, or let the algorithm learn the ideal stall threshold value itself through the stall learning process.

User-Defined Stall Threshold: Users can write a value to the threshold register if they have torque count information for their use case. They can get torque count information for their use case by reading the TRQ_COUNT register, during normal operation of the motor and when the motor is stalled. The stall threshold should be set as the average of steady count and stall count. The characterization of the torque count should be done over the entire range of operating conditions (temperature, supply voltage, speed, and so forth) and for both directions of motion.

If the operating conditions vary a lot, such as the motor speed changing between high and low values, it may not be possible to set a single stall threshold for all conditions. In this case, the controller may implement a look-up table for the stall threshold. Sometimes, an external low-pass filter with a sufficiently high time-constant might be needed to remove ripples in the torque count due to vibration when the motor is stalled.

Driver-Defined Stall Threshold: The system itself can go into stall learning mode and calculate the ideal stall threshold for the motor. The following procedure describes the stall learning mode:

- Run motor on no load
- Initiate learning by writing STL_LRN = 1
- Wait for 32 electrical cycles for the driver to learn the steady count. The time to wait will depend on the step frequency and microstepping.
- Stall the motor
- Wait for 16 electrical cycles for the driver to learn the stall count
- Read the register until STL_LRN = 0
- If STL_LRN_OK = 1, then the stall threshold value has been calculated. If STL_LRN_OK = 0, then the stall learning is not successful.
- Stall threshold is calculated as the average of steady count and stall count. At the end of a successful learning, the STALL_TH register is loaded with the proper stall threshold bits.

Sometimes the stall learning process might not be successful due to an unstable torque count while the motor is running or stalled. For example, as detailed in Section 7, when the motor has high coil resistance or is running at very high or low speeds, the torque count might vary by a lot over time and the difference between steady count and stall count might be small. In such cases, it is recommended to not use the stall learning method. Instead, the user should carefully study the steady count and torque count across the range of operating conditions and set the threshold midway between the minimum steady count and the maximum stall count.

7 Torque Count Variation With Operating Conditions

Torque count is fairly constant across variations of supply voltage, temperature, and other operating conditions. However, second-order effects will cause small variations in the torque count value, as detailed in this section.

7.1 Variation With Motor Speed and Direction of Motion

Torque count may vary with the direction of motion of the motor. The effective loading of the motor sometimes depends on the direction of the movement. For example, in some cases, the rotor movement might be assisted by gravity or coil spring in one direction and opposed in the other direction. Differences in loading cause different phase changes of back EMF with respect to the coil current. This results in different steady counts, depending on the direction of motion.
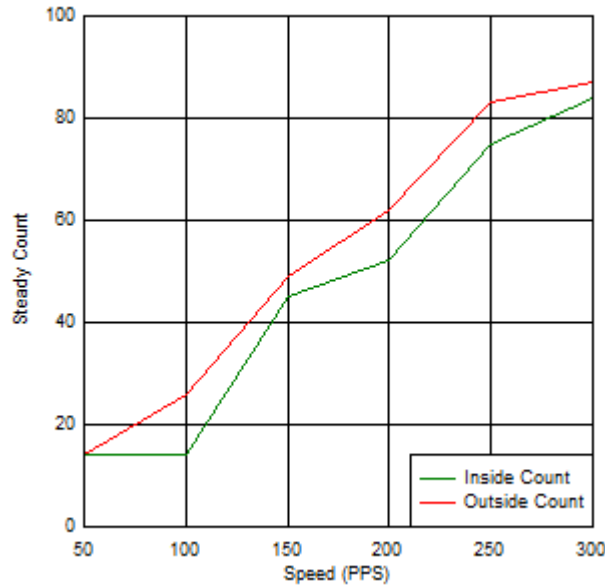
Figure 9. Steady Count Variation With Speed for Different Directions of Motion

Figure 9 shows how the steady count of the PL35L-024 motor changes depending on whether the rotor shaft is moving inside or outside. The motor was operating in full step mode, the full-scale current was set at 200 mA and the slew rate was 105 V/µs. The supply voltage was 13.5 V. Note that the steady count almost linearly increases with motor speed. This is because, the back EMF is directly proportional to motor speed. More back EMF at higher speed results in larger differences to the T_{OFF}s between rising and falling current quadrants - in other words, a larger torque count.
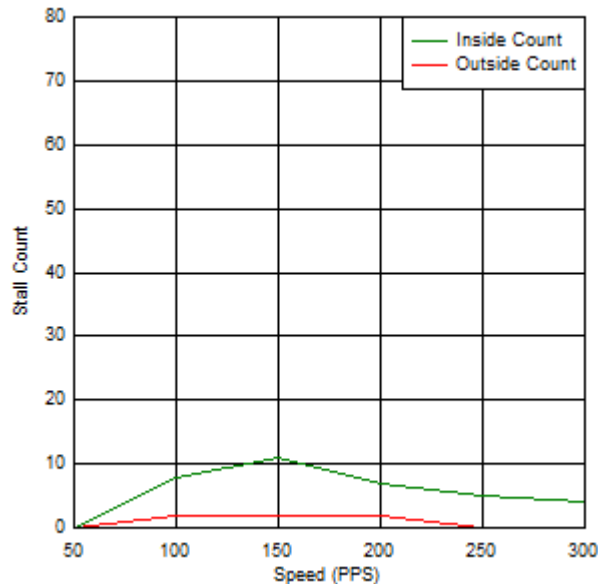

Figure 10. Stall Count Variation With Direction of Motion

The torque count when the motor is stalled (stall count) may also vary with the direction of motion. Stall count depends on the hardness of the end-stop. The end of travel may not actually stall the rotor - in some cases, the rotor may continue spinning due to a loose, spongy, or soft end-stop which allows the rotor to bounce. Typically, a stalled rotor vibrates as it tries to move; however, any rotational movement translates to back EMF. Motors with large step angles may display more vibration than motors with smaller step angles. In such cases, stall count will be definitely lower than steady count, but it may not be zero. Figure 10 shows the stall count of the PL35L-024 motor for the same operating conditions.
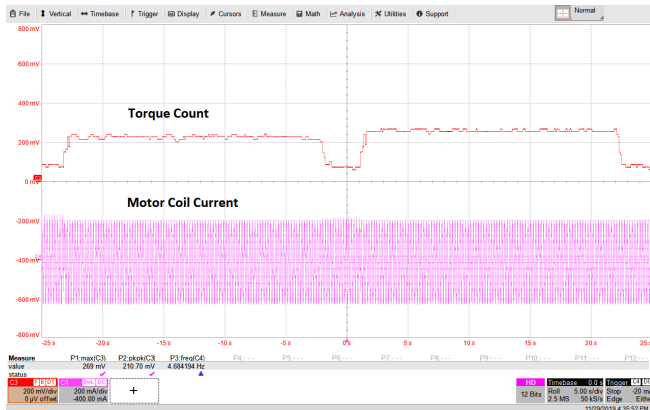
7.1.1   Limitations Due to Low Motor Speed
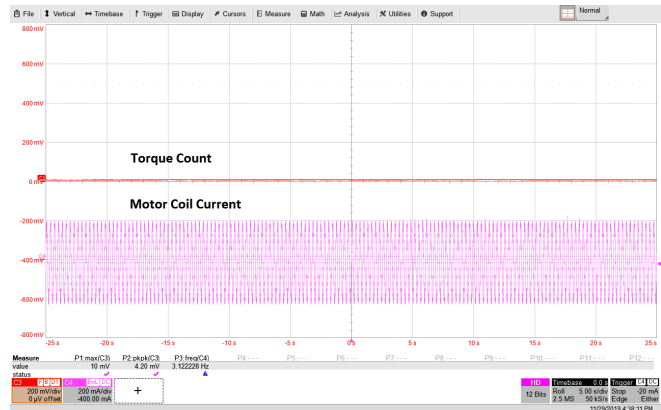

Figure 11. Steady Count at 150 pps

Figure 12. Steady Count at 100 pps

Figure 11 and Figure 12 show the torque count of the PL35L motor at low speeds. While the motor is set to run at 1/8 microstepping, at 150 pps speed, torque count is significantly lower than the counts at 1000 pps for both directions of motion, but a proper stall threshold can still be selected for reliable stall detection. However, when the motor speed is further reduced to 100 pps, torque count becomes close to zero. This is because, at low speeds, back EMF is also proportionally low and it may not be enough to cause any perceptible change in T_{OFF} between the rising and falling quadrants. Therefore, the DRV8889-Q1 will not be able to detect stall at ultra-low speeds.

7.1.2   Limitations Due to High Motor Speed

High speed, and large back EMF distorts the coil current and stall detection might be unreliable at very high motor speeds. The following four scope shots show the coil current in full step mode for a 17PM-F438B motor, running with 13.5-V supply voltage and 500-mA full-scale current.

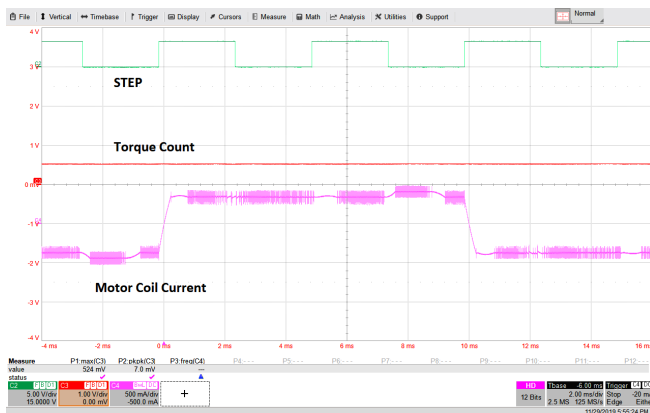**Figure 13. Steady Count at 200 pps**

Figure 14. Steady Count at 700 pps

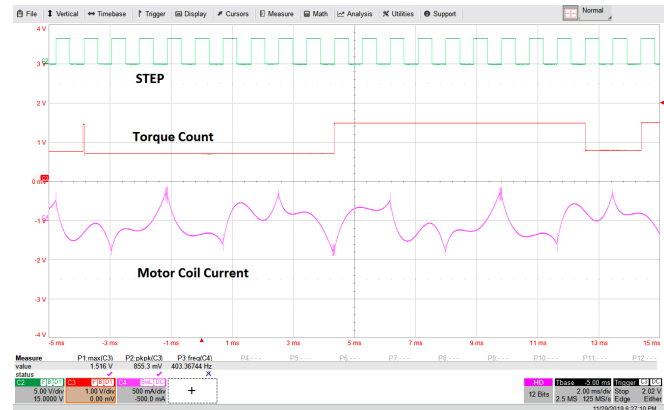Figure 15. Steady Count Change When Q1 Regulation is Lost

Figure 16. Steady Count at 1100 pps

As Figure 13 shows, when the motor speed is such that current is regulated in both Q1 and Q2 quadrants, the algorithm uses the T_{OFF} from both quadrants and derives the torque count.

Figure 14 shows that at higher speeds, the rise time of the current can be so high that current regulation in Q1 will be lost, but current will still be regulated in Q2. Even in this case, stall can still be detected reliably. When current regulation is lost in Q1, it causes a sudden jump in the torque count value, as Figure 15 shows.

At even higher speeds (Figure 16), the current waveform might be so highly distorted that regulation will be lost in both Q1 and Q2 quadrants. In such cases, the algorithm can no longer detect stall and the torque count value will be unstable and unreliable.

The rise time of the current, shown in Figure 14, depends on the supply voltage, coil inductance, and coil current level according to the well-known $V = L \times dI/dt$ equation. Lower rise time allows the current to be regulated at even higher speeds. Therefore, wider operating speed range can be obtained through, (1) a motor with low inductance, (2) lower current level, and (3) higher supply voltage.
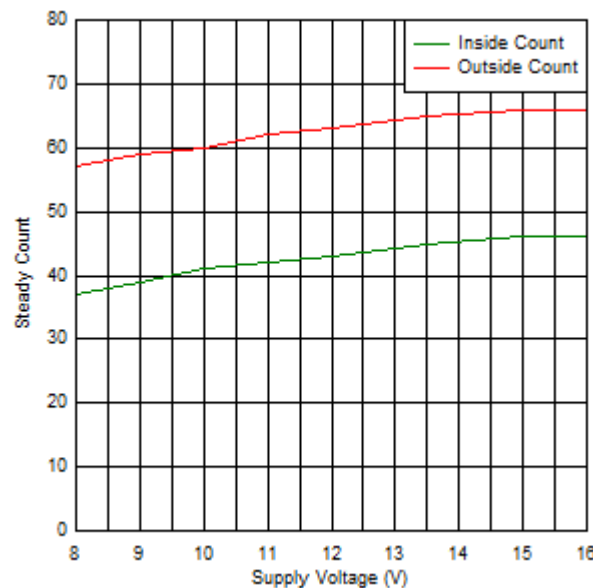
7.2 Variation With Supply Voltage

Figure 17. Steady Count Variation With Supply Voltage

Equation 5 states that the T_{OFF} parameter is independent of supply voltage (VM). Therefore, when the average of T_{OFF} from one quadrant is compared to the average of T_{OFF} from the next quadrant, the result should be independent of supply voltage. However, Figure 17 shows that there is small variation in the steady count with supply voltage. This data is for the PL35L-024 motor, at 1/8 microstepping with 1000 pps speed, 105 V/µs slew rate, and full-scale current set at 200 mA.

This variation can be explained by looking at the current ripple at various supply voltages. At higher voltages, the ripple increases slightly, which results in a slight increase in the T_{OFF} value. However, the change in T_{OFF} for the Q2 quadrant will be slightly larger than the T_{OFF} change in Q1, because the back-EMF magnitude remains constant at higher voltages. The effect of this is the slight increase in steady count with supply voltage.
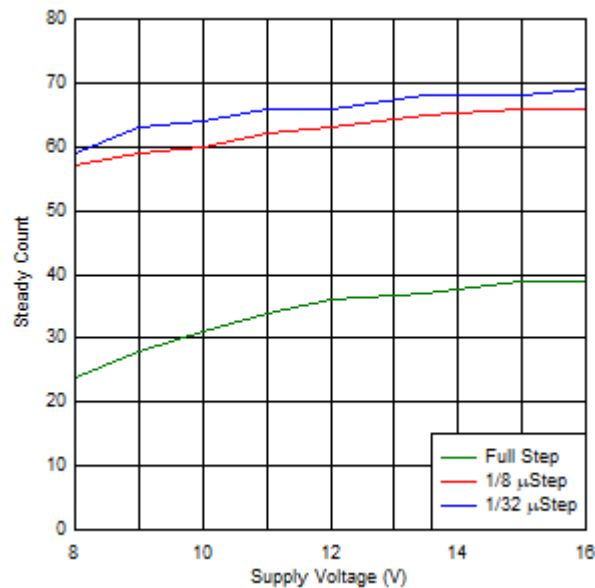
7.3 Variation With Microstepping Setting

Figure 18. Steady Count Variation With Microstepping

Higher-order microstepping generally results in a higher torque count. Figure 18 shows the variation in steady count with microstepping settings for the PL35L-024 motor. The motor speed (pps) was adjusted at each microstepping to arrive at the same 125 full steps per second rate.
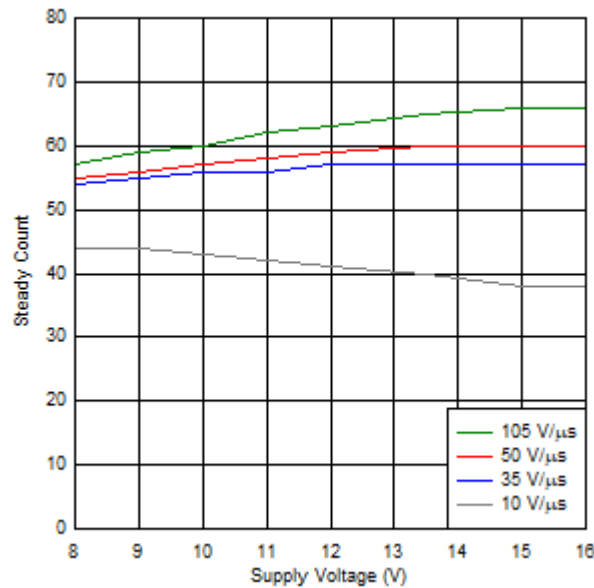
7.4 Variation With Output Slew Rate

Figure 19. Steady Count Variation With Output Slew Rate

Slower output slew rate results in a lower torque count. Due to slower output fall time, the T_{OFF} decreases at a slower slew rate, which leads to lower torque count.

Higher slew rates are also preferable to keep the switching loss of the driver to a minimum - allows the driver to support higher currents at a given ambient temperature. Conversely, lower slew rates result in better EMC performance. A careful trade-off analysis needs to be carried out to select the proper slew rate for an application.

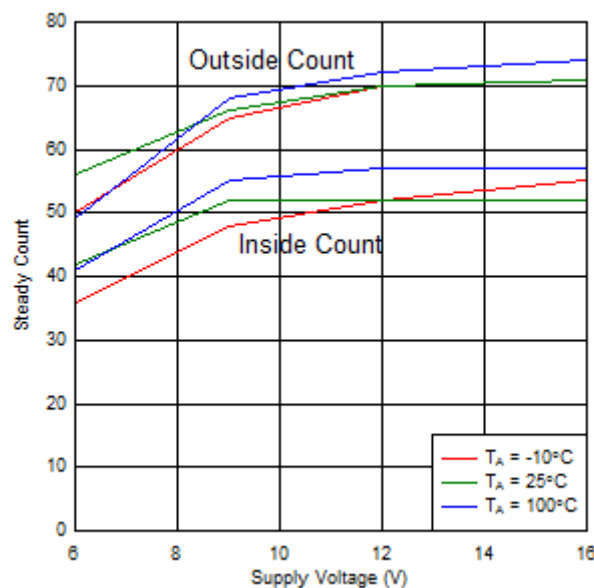## 7.5 Variation With Ambient Temperature

Figure 20. Steady Count Variation With Ambient Temperature

Figure 20 shows how the inside and outside counts change with ambient temperature for a stepper used in a HVAC gas valve. The motor was running at full-step mode with 300 pps speed. As is evident from the plot, the torque count is almost independent of the ambient temperature.

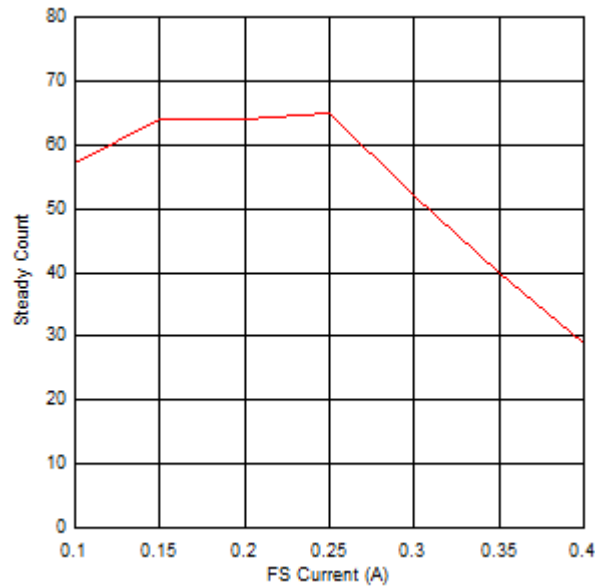## 7.6 Variation With Full-Scale Current Setting

Figure 21. Steady Count Variation With Full-scale Current

At a constant supply voltage, steady count drops at higher full-scale current. High $I \times R_{coil}$ drop across the motor coil leaves too little back EMF; therefore, the T_{OFF} does not get affected, causing lower count.

7.6.1 Limitations Due to High Coil Resistance

If the coil resistance is too high, the coil current waveform is distorted and the back EMF is unable to influence the T_{OFF} - resulting in unreliable torque count and stall detection.
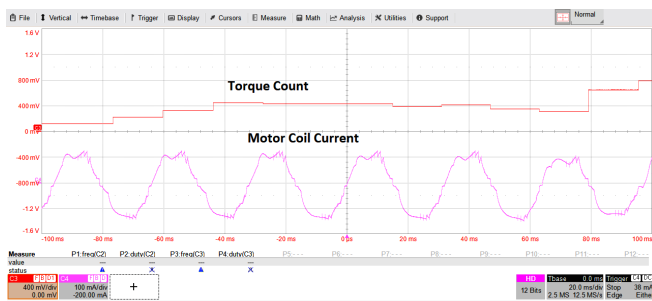

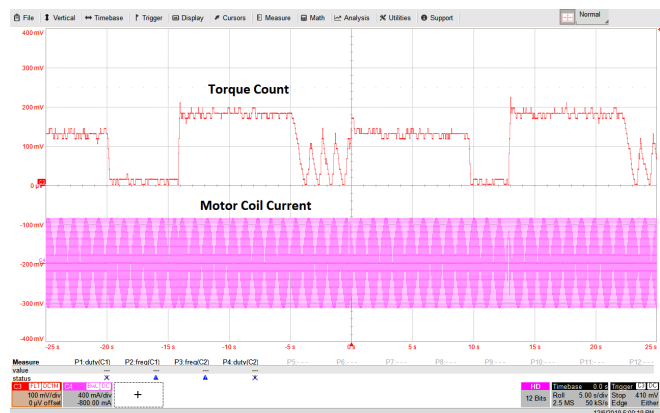**Figure 22. Coil Current Waveform for a Valve Motor With 80-Ω Resistance**

Figure 23. Coil Current Waveform for a Valve Motor With 36-Ω Resistance

Figure 22 shows the coil current waveform for an HVAC valve motor with 80–Ω resistance. The supply voltage was 12 V, and the full scale current was 200 mA. It is clear that the torque count waveform is erratic in nature and a stall cannot be reliably detected. Figure 23 shows the torque count for another HVAC motor with 36–Ω coil resistance at the same operating condition. When the motor is stalled at one end, there is periodic vibration - leading to spikes in the stall count. Even though there is some overlap between steady count and stall count, using an external low-pass filter with sufficiently high time-constant to eliminate the spikes in the stall count can result in reliable stall detection.

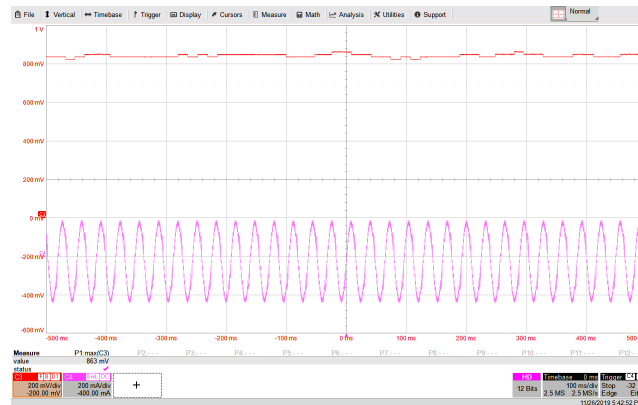## 7.7 *Steady-State Count Variation at a Fixed Operating Condition*

Figure 24. Steady-State Torque Count Variation

Figure 24 shows the steady count of the PL35L-024 motor, running at 1/8 microstepping and 1000 pps speed. The waveform has a peak-to-peak ripple of 42 mV, corresponding to a count variation by 3. In other words, steady count is varying between 63 and 66. This can be explained by small random variations in the T_{OFF} due to several factors - such as the nature of the back-EMF voltage and minor asymmetries in motor construction.

8 Evaluation Examples

8.1 *Automotive Headlight Leveling and Swivel*

Adaptive front lighting (AFS) systems are increasingly being adopted by car manufacturers across geographical locations. These systems compensate for changes in the inclination of the vehicle relative to the road surface by making slight vertical adjustments to the light beam of the headlamp. They also cause the headlamps to swivel in response to a change in the turning direction of the vehicle. Stepper motors are often used for headlamp adjustment applications because stepper motors are low cost, rugged, and provide a high torque in relation to their size.

Most automotive headlamp systems require stall detection, to prevent the motor from hitting end-stop during the initial position calibration or during normal operation. Without stall detection, to ensure that the end-stop is reached, the stepper motor is driven multiple steps beyond the estimated end-stop position. This results in a blocked motor with associated audible noise and mechanical wear-out. Audible noise is particularly sensitive for electric vehicles. Without integrated stall detection, some systems are forced to use expensive position sensors to receive feedback about the angular location of the motor.

The following example shows how the DRV8889-Q1 detects stall for an automotive headlight module. This headlight module uses a PL35L-A24 stepper motor. While running, the rotor shaft moves inside or outside and can get stalled at both ends. The operating conditions for this typical adaptive headlight application are listed in Table 2.

Table 2. Operating Conditions for Headlight Stepper Motor

Parameter	Value
Supply voltage range	9 V to 16 V

Table 2. Operating Conditions for Headlight Stepper Motor (continued)

Parameter	Value
Full scale current	500 mA
Target speed	122.5 Full-steps/s
Microstepping	1/8 or 1/32
Temperature range	-40°C to 105°C
Motor coil resistance	7.7 Ω
Motor step angle	15°
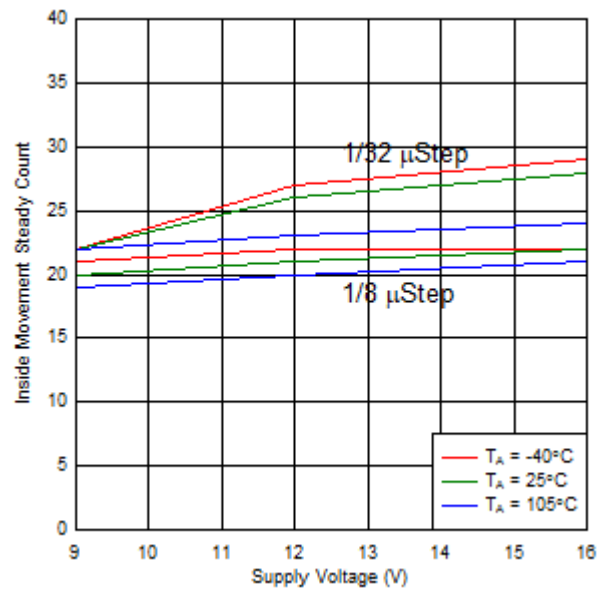
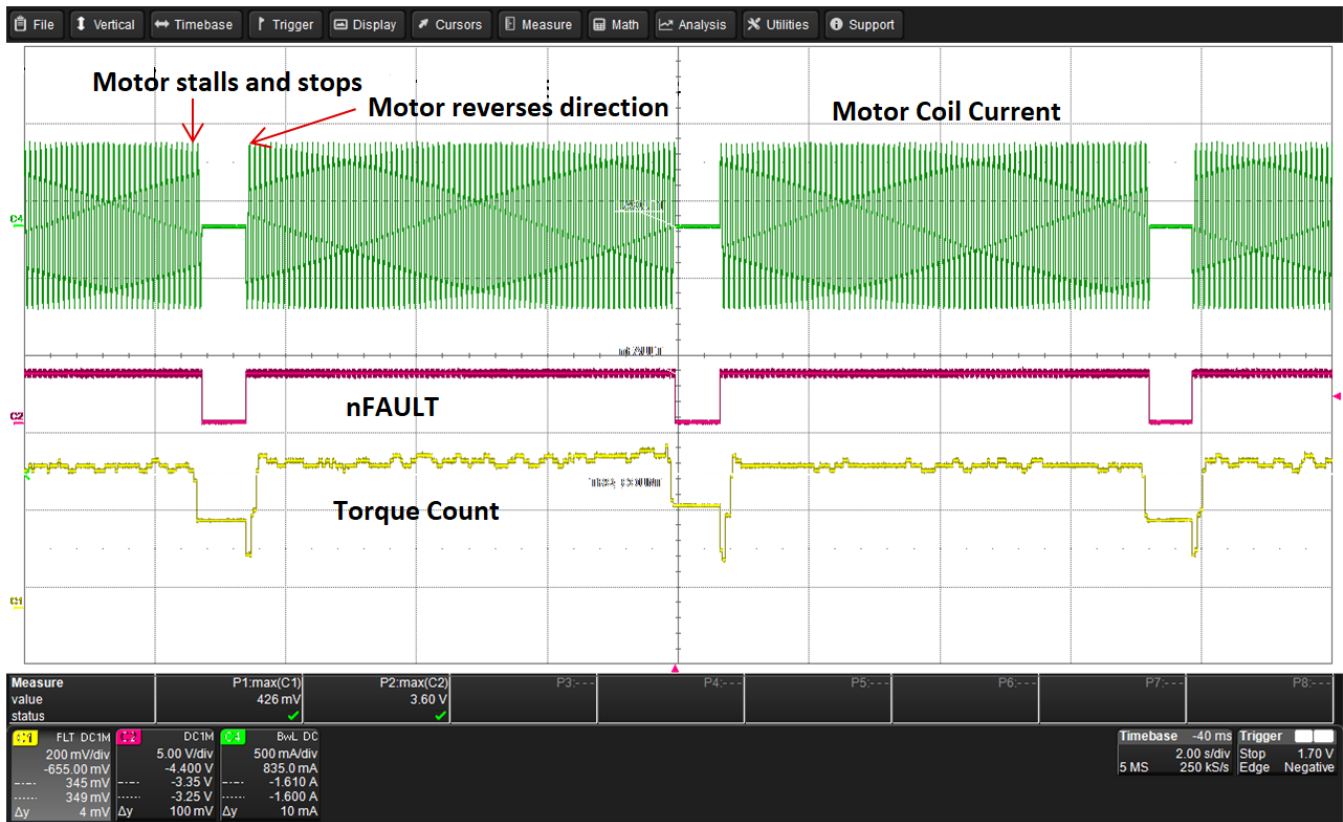**Figure 25. Steady Count Across Operating Conditions**

Figure 26. Stall Detection of a Headlight Module With DRV8889-Q1

Figure 25 plots the steady count for the inside movement as a function of the operational parameters of the headlight module. The inside direction count is lower than the outside direction count. Based on the minimum inside count, choose a stall threshold of 12. With this stall threshold, the DRV8889-Q1 detects stall reliably at both ends of operation across operating conditions, as Figure 26 shows. The nFAULT output goes low whenever the torque count is lower than the stall threshold, indicating to the system that stall has been detected.
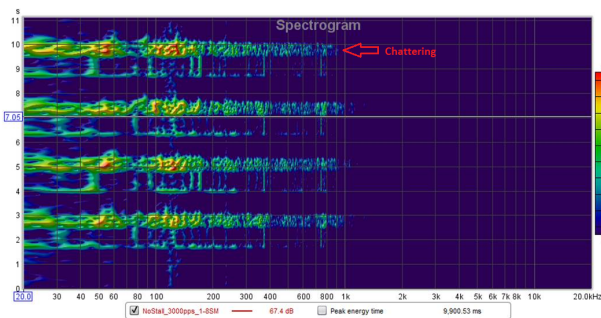

Figure 27. Audio Noise Spectrogram Without Stall Detection
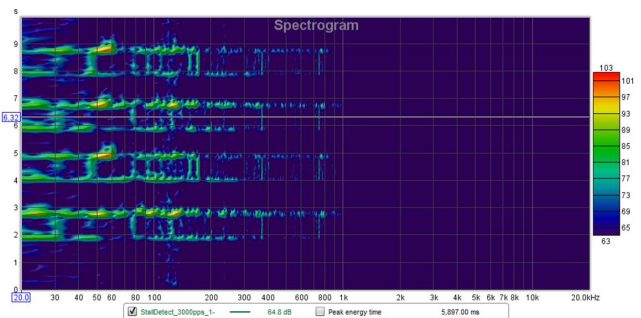

Figure 28. Audio Noise Spectrogram With DRV8889-Q1 Stall Detection

Figure 27 and Figure 28 show the audio noise spectrograms for two cases – one in which the headlight module operates without stall detection and the other in which the module uses the DRV8889-Q1 device to detect stall at both ends. Figure 27 clearly shows the evidence of large audio noise at approximately 55 Hz and between 100 Hz and 200 Hz. This spectrogram also shows how the stepper motor chatters when it reaches the end-of-line – an effect of the over-drive needed to ensure that the motor has indeed reached the end. Conversely, Figure 28 shows that the audio noise is largely absent – more so between 100 Hz and 200 Hz, and the chattering is also non-existent.
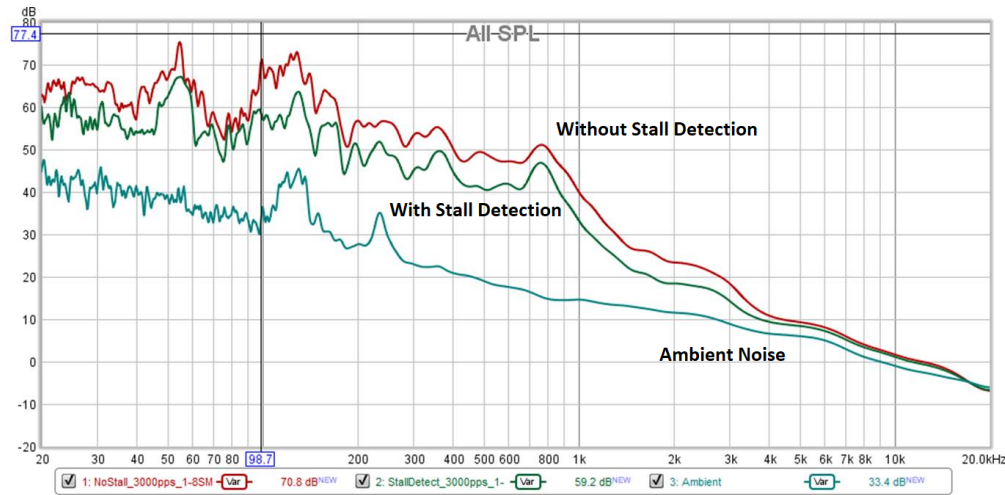

Figure 29. Audio Noise SPL Plot With and Without Stall Detection

Figure 29 also compares the audio noise for the two cases. The plot in red corresponds to audio noise without stall detection, and the plot in green is when the stall detection algorithm of the DRV8889-Q1 is used. Clearly, with stall detection, there is more than 10-dB improvement in the noise level at some frequencies.

8.2 Automotive Head-up Display (HUD)

Automotive Head-Up Displays (HUD) are currently available in various medium and high-end cars and also as after-market products. A HUD display is intended to assist drivers by projecting important trip information such as speed, navigation data, RPM, alerts, and augmented reality overlays onto the inside surface of the windshield or a transparent piece of plastic called a 'combiner'. The system requires multiple lenses and mirrors to project the information onto the windshield or combiner, and the mirrors must be rotated with precision to achieve accurate positioning. Therefore, a lot of HUD units use stepper motors, and sensorless stall detection is often a requirement to ensure that the mirrors reach their end stop without resulting in excessive audio noise or mechanical wear-out.

The following example shows how the DRV8889-Q1 device detects stall for an automotive HUD module. This combiner HUD module uses a custom bipolar stepper motor, which moves a reflector mirror up and down. The operating conditions of the HUD application and details of the stepper motor are shown in Table 3.

Table 3. Operating Conditions for HUD Module

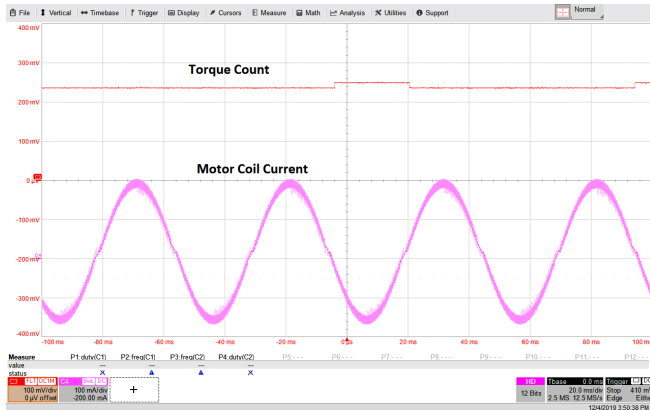| Parameter	Value
Operating voltage range	8 V to 16 V
Full-scale current	180 mA
Target speed	2550 pps
Microstepping	1/32
Temperature range	-40°C to +85°C
Motor coil resistance	20 Ω ±7%
Step angle	0.514° / STEP

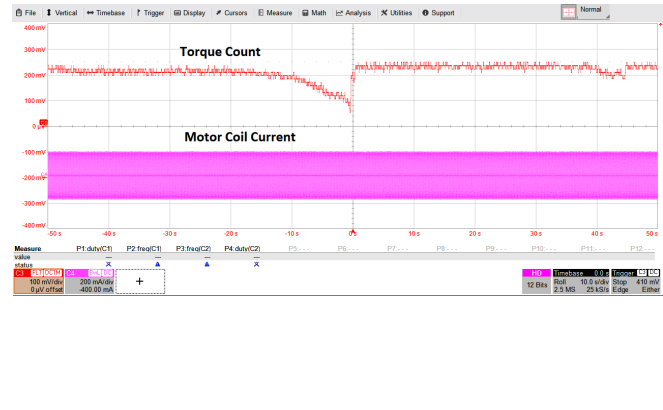**Figure 30. HUD Module Running at 12 V With 1/32 Microstepping**

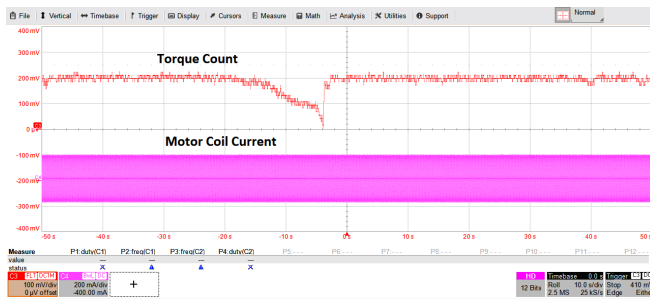**Figure 31. Stall Detection at 12 V**

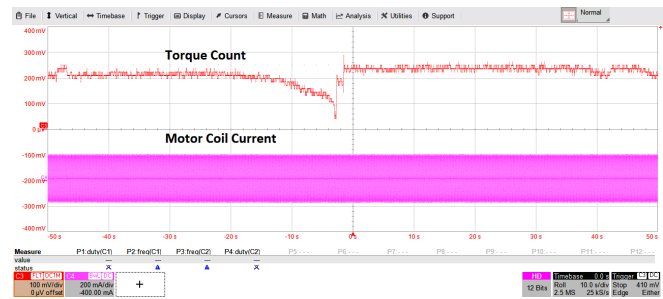**Figure 32. Stall Detection at 8 V**

Figure 33. Stall Detection at 16 V

Figure 31 to Figure 33 show how the torque count decreases during motor stall at various voltages. A common stall threshold such as 120 mV (corresponding to TRQ_COUNT = 10) will detect stall reliably across corners for this application.

8.3 HVAC Valve Control

HVAC valve control actuators also require stall detection. A stepper motor driver with integrated sensorless stall algorithm allows precise detection of the end-stop of a flap or a valve tip in an HVAC system, without requiring over-drive of the stepper motor. The following example shows how the DRV8889-Q1 detects stall for an HVAC valve. The operating conditions of this HVAC application are shown in Table 3.

Table 4. Operating Conditions for HVAC Valve

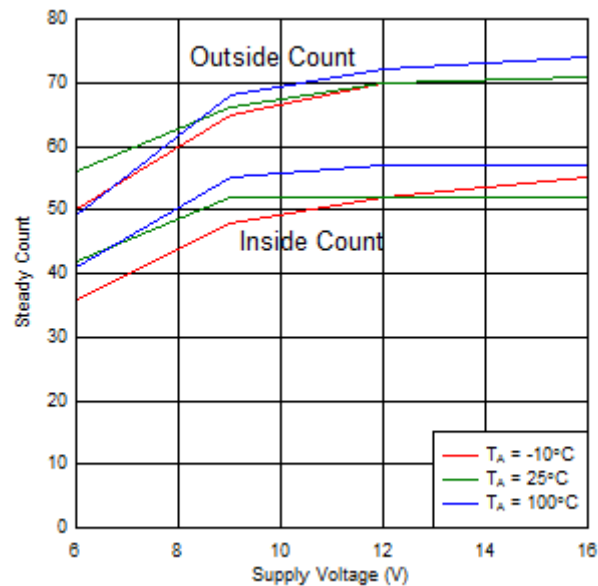| Parameter	Value
Operating Voltage Range	6 V to 16 V
Full Scale Current	300 mA
Target Speed	300 steps/sec
Microstepping	Full-step
Temperature range	-30 °C to +100 °C

Figure 34. HVAC Valve Steady Count

The valve motor gets stalled at both ends of the movement. Figure 34 shows the steady count in both directions as a function of the supply voltage. A stall threshold of 30 works well to reliably detect stall at both the ends of the valve tip movement.

9 Conclusion

Various sensorless stall detection algorithms are available in the market from different manufacturers. The novel stall detection algorithm implemented in the DRV8889-Q1 device can reliably detect stall for various applications over a wide range of supply voltage, speed, and other operational parameters. The robustness of the algorithm, combined with the ease of use, makes the DRV8889-Q1 an ideal option to replace costly position sensors used to send positional feedback in a wide range of end applications.

10 References

For additional reference, refer to the following:
- Acarnley, Paul P. *Stepping motors: a guide to theory and practice.* 4th ed., Institution of Engineering and Technology, 2007.
- Methods and apparatus for robust and efficient stepper motor BEMF measurement, by Sooping Saw, Rakesh Raja, Anuj Jain and Matthew Hein; United States Patent US10063170B2
- Stall detection in stepper motors using differential back-emf between rising and falling commutation phase of motor current, by Sooping Saw, Rakesh Raja, Wen Pin Lin and Sudhir Nagaraj; United States Patent US20190109551A1
- Texas Instruments, *DRV8889-Q1 Automotive Stepper Driver with Integrated Current Sense, 1/256 Micro-Stepping, and Stall Detection Data Sheet*

IMPORTANT NOTICE AND DISCLAIMER

TI PROVIDES TECHNICAL AND RELIABILITY DATA (INCLUDING DATA SHEETS), DESIGN RESOURCES (INCLUDING REFERENCE DESIGNS), APPLICATION OR OTHER DESIGN ADVICE, WEB TOOLS, SAFETY INFORMATION, AND OTHER RESOURCES "AS IS" AND WITH ALL FAULTS, AND DISCLAIMS ALL WARRANTIES, EXPRESS AND IMPLIED, INCLUDING WITHOUT LIMITATION ANY IMPLIED WARRANTIES OF MERCHANTABILITY, FITNESS FOR A PARTICULAR PURPOSE OR NON-INFRINGEMENT OF THIRD PARTY INTELLECTUAL PROPERTY RIGHTS.

These resources are intended for skilled developers designing with TI products. You are solely responsible for (1) selecting the appropriate TI products for your application, (2) designing, validating and testing your application, and (3) ensuring your application meets applicable standards, and any other safety, security, regulatory or other requirements.

These resources are subject to change without notice. TI grants you permission to use these resources only for development of an application that uses the TI products described in the resource. Other reproduction and display of these resources is prohibited. No license is granted to any other TI intellectual property right or to any third party intellectual property right. TI disclaims responsibility for, and you will fully indemnify TI and its representatives against, any claims, damages, costs, losses, and liabilities arising out of your use of these resources.

TI's products are provided subject to TI's Terms of Sale or other applicable terms available either on ti.com or provided in conjunction with such TI products. TI's provision of these resources does not expand or otherwise alter TI's applicable warranties or warranty disclaimers for TI products.

TI objects to and rejects any additional or different terms you may have proposed.

Mailing Address: Texas Instruments, Post Office Box 655303, Dallas, Texas 75265
Copyright © 2022, Texas Instruments Incorporated